Superconducting and hybrid systems for magnetic field shielding

Superconductor Science and Technology 29 (3), 034004 (2016)

DOI: 10.1088/0953-2048/29/3/034004

Superconducting and hybrid systems for magnetic field shielding

L. Gozzelino [1,2], R. Gerbaldo [1,2], G. Ghigo [1,2], F. Laviano [1,2], M. Truccato[2,3], A. Agostino[4]

[1] *Department of Applied Science and Technology, Politecnico di Torino, Torino, Italy*
[2] *Istituto Nazionale di Fisica Nucleare, Sezione di Torino, Torino Italy*
[3] *Department of Physics, University of Torino, Torino, Italy*
[4] *Department of Chemistry, University of Torino, Torino, Italy*

Abstract

In this paper we investigate and compare the shielding properties of superconducting and hybrid superconducting/ferromagnetic systems, consisting in cylindrical cups with aspect ratio height/radius close to unity. Firstly, we reproduced by finite element calculations the induction magnetic field values measured along the symmetry axis in a superconducting (MgB_2) and in a hybrid configuration (MgB_2/Fe) as a function of the applied magnetic field and of the position. The calculations were carried out using the vector potential formalism, taking into account simultaneously the non-linear properties of both the superconducting and the ferromagnetic material. On the basis of the good agreement between the experimental and the computed data we applied the same model to study the influence of the geometrical parameters of the ferromagnetic cup as well as of the thickness of the lateral gap between the two cups on the shielding properties of the superconducting cup. The results show that in the considered non-ideal geometry, where the edge effect in the flux penetration cannot be disregarded, the superconducting shield is always the most efficient solution at low magnetic fields. However, a partial recovery of the shielding capability of the hybrid configuration occurs if a mismatch in the open edges of the two cups is considered. On the contrary, at high magnetic fields the hybrid configurations are always the most effective. In particular, the highest shielding factor was found for solutions with the ferromagnetic cup protruding over the superconducting one.

1. Introduction

Shielding of magnetic fields is crucial for several applications requiring an ultralow magnetic field environment (e.g. biomedical application) or the mitigation of the magnetic field produced by an electronic device in order to guarantee the electromagnetic compatibility with the surrounding environment or to reduce the device electromagnetic signature (e.g. electromagnetic compatibility between different equipments or military applications).

For their electromagnetic properties, superconducting (SC) and ferromagnetic (FM) materials are the natural candidates for passive magnetic shields in the low-frequency field range. Among the superconductors, both low-temperature superconductors [1, 2], high-temperature superconducting cuprates [3, 4] and MgB_2 [5, 6] were successfully employed for passive shields. Moreover, in the last decade, the investigations on the combined use of superconducting and ferromagnetic materials in passive shielding have led to promising experimental results [6-11] including the cloaking of dc and ac magnetic fields [12-14].

In addition, the parallel development of numerical codes allowed addressing complex problems, such as the distribution of the current density and of the induction magnetic field inside superconductors of several geometries [15-18], even in presence of other materials with nonlinear magnetic properties, such as ferromagnets [14, 19-21]. Several methods have been proposed for the superconducting modeling [15, 22] where the problem is expressed in terms of the field variables (e.g. the so-called **H** formalism [23]) or in terms of potentials (e.g. the **A** – V formalism [24]). In this framework, an interesting approach was proposed by A. Campbell [25, 26] that resolves the evolution of critical state in a hard superconductor using a force-displacement method. Following this approach, F. Gömöry *et al.* [27] developed a procedure based on the **A**-V formalism, successfully applied for the calculations of the magnetic flux penetration into SC/FM composites with nonlinear properties of the superconducting and the magnetic layers.

In previous papers we have studied experimentally the shielding properties of a hybrid MgB_2/Fe structure consisting in two coaxial cylindrical cups, subjected to an external magnetic field parallel to its axis [6, 11]. Height and radius of each cup were chosen of similar values in order to analyze the shielding potential of the materials in a situation where it is necessary to minimize the amount of space occupied by the shield. In such a configuration, the field penetration through the open end cannot be neglected. The magnetic field mitigation was investigated in a magnetic field range up to 1.5 T, as a function of the external source field and of the position along the cup axis. It turned out that, at T = 20 K and at higher applied fields, the shielding efficiency of the hybrid system overcomes by more than a factor three that of the single MgB_2 cup whereas, at low field, the only superconducting solution is the most efficient.

In this paper we extend the previous study of [6, 11]. The final aim is the improvement of the shielding properties in cup-shaped shields with aspect ratio similar to that of the MgB_2/Fe system experimentally investigated by means of a suitable sizing of the superconducting and ferromagnetic sheets. Previous calculations on hybrid shields carried out by Lousberg et al. [19] highlighted the influence of the ferromagnetic layer position and size on the shielding efficiency of a superconducting tube. Moreover, also the lateral air gap size was demonstrated to affect the shielding performance of tubular hybrid systems [7, 8]. However, these previous investigations concerned samples with an aspect ratio height/radius higher than 10 and focused on the induction field values in the tube center, i.e. in a position where the field penetration from the open ends can be disregarded.

We firstly reproduced by computation the experimental behaviors of the induction field previously measured along the axis of the superconducting and the hybrid shields. The simulations were performed using the vector potential formulation proposed in [27]. The superconductor is modeled through its non-linear $J_c(B)$ dependence and the ferromagnet through its B-H curve. Afterwards, numerical simulations were performed on similar coaxial systems in order to investigate how the geometrical parameters of the ferromagnetic cup as well as the thickness of the lateral gap between the two cups can affect the shielding properties of the superconducting sample. The behavior of the magnetic induction is calculated along the cup axis, both inside and outside the cups, as a function of the position and for several applied field.

The paper is organized as follows. In Section 2 we briefly remind the details of the magnetic shielding measurements and describe the numerical model used for the calculation of the induction magnetic field values. The comparison between the experimental data and the simulation outputs are reported in Section 3, while in Section 4 we present and discuss the numerical results obtained by changing the geometric parameters of the hybrid shield. The main outcomes are finally summarized in Section 5.

2. Experimental details and numerical model

2.1 Measurement details

The MgB_2 and Fe cups were placed on the top of a cooling stage of a cryogen-free cryocooler. MgB_2 was grown by a microwave heating-assisted Mg-RLI (Mg Reactive Liquid Infiltration) technique in B preforms [28] as detailed elsewhere [6]. The additional microwave heating [29] allows the minimization of the magnesium amount in the matrix of the material, reducing the

chemical reactivity and the instability of the system. Fe cup was made out of a commercial ARMCO-iron suitably degaussed before each set of measurements.

The magnetic field was applied parallel to the cup axis (*z*-axis). The axial component of the induction magnetic field, B_z, was measured by a high sensitivity cryogenic Hall probe, mounted on the bottom surface of a custom-designed motor-driven stage, able to be moved along the axis of the cups with a spatial resolution of 1 μm [30]. Firstly we measured the shielding properties of the single MgB_2 cup, then of the hybrid system with the MgB_2 cup placed inside the ferromagnetic one, as shown in Fig. 1, where the cup sizes are also reported. In this configuration the edge of both the cups are at the same level and a gap of 1 mm separate the outer lateral surface of the SC cup from the inner lateral surface of the FM one.

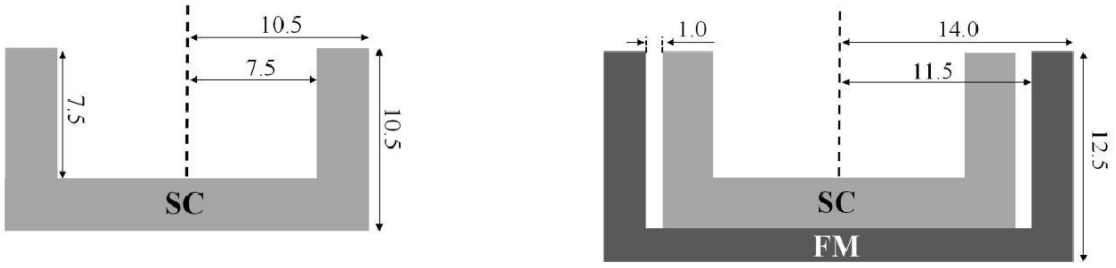

Figure 1. Schematic view of the MgB_2 cup and of the MgB_2/Fe cup arrangement characterized experimentally. All the sizes are in mm.

2.2 Numerical model for the computation of the induction magnetic field distribution

Simulations were performed by a commercial finite-element software [31]. The studied system is made of three domains: the superconductor domain, the ferromagnetic domain and the vacuum domain. The source term for the magnetic field is represented through the boundary conditions.

The evolution of the magnetic field distribution inside the superconducting layer was calculated following the formulation based on the idea of A. Campbell [25] in the form proposed by F. Gömöry *et al.* [27]. The equation to be solved is $\mathbf{J} = \nabla \times \mathbf{B}\,\mu = \nabla \times \left(\frac{1}{\mu} \nabla \times \mathbf{A}\right)$ where **J** is the macroscopic current supported by the superconductor, μ is the magnetic permeability (assumed equal to μ_0, the vacuum magnetic permeability) and **A** is the vector potential. Since the MgB_2 cup is polycrystalline, its magnetic properties were considered isotropic. Here, **A** is the independent variable and the key element of this simulation approach is the relationship between the supercurrent density and the vector potential, whose value was set to zero in the so-called neutral zone (i.e. the zone where the electric field always vanishes). Moreover, the magnetic flux was

assumed to penetrate monotonically from the SC/FM surface when the applied field changes monotonically.

Taking into account the axisymmetric geometry of the problem, we worked in cylindrical coordinates. As the applied field is directed in the *z*-direction, i.e. along the cup axis, the vector potential has only one component, $\mathbf{A}(r, z) = A_\phi(r, z)\mathbf{u}_\phi$, and the magnetic induction is invariant under a rotation around the *z*-axis and has no ϕ-component: $\mathbf{B}(r, z) = \nabla \times \mathbf{A}(r, z) = B_r(r, z)\mathbf{u_r} + B_z(r, z)\mathbf{u}_z$. Here $\mathbf{u}_r$, $\mathbf{u}_\phi$ and $\mathbf{u}_z$ are the unit vectors along the *r*-, ϕ- and *z*-directions, respectively.

The induction field distribution was calculated for applied fields monotonically increasing up the maximum value $\mu_0 H_{max}$ =1.5 T. Starting from the virgin state, we assumed the initial condition A_ϕ = 0 everywhere and imposed a current density flowing in the superconductor and fulfilling the equation:

$$j_\phi(r, z) = j_c \left(\frac{-A_\phi(r, z)}{A_n} \right)$$

where j_c is the critical current density and A_n is a scaling factor affecting the shape of the current distribution inside the superconductor [27]. We assumed $A_n = 5 \cdot 10^{-8}$ Wb/m. It is worth mentioning that, since the current density is parallel to the vector potential, it has only the ϕ-component.

Since the induction field dependence of the critical current cannot be disregarded, we assumed the following J_c dependence [32]:

$$J_c(B) = K \left(\frac{B}{B_{irr}} \right)^\gamma \left(1 - \frac{B}{B_{irr}} \right)^\delta \quad (1)$$

where γ and δ are parameters depending on the pinning typology [33] and B_{irr} is the irreversibility field.

The magnetic flux penetration in the Fe cups was evaluated using the material constitutive law induction vs. applied magnetic field [34].

The vacuum domain was drawn as a coaxial cylinder with a radius, R_v, 10 times larger than the ferromagnetic cup radius. Working in the Coulomb gauge, since the external magnetic field was applied parallel to the *z*-axis, the vector potential was required to satisfy the following condition: $A_\phi(r, z) = \frac{\mu_0 H_{appl} \times R_v}{2}$ on the lateral surface of the cylinder and $A_\phi(r, z) = \frac{\mu_0 H_{appl} \times r}{2}$ on its bases, where r is the distance for the system axis.

3. Comparison between the experimental results and the numerical simulation outputs

In Fig. 2 the values of the induction magnetic field measured at T = 20 K inside the superconducting cup and the hybrid system, at a distance of 5.5 mm from the cup edge, are compared with those calculated with the procedure described in the previous section. To model the superconducting material, the following parameters were used in Eq. 1: K = $1.16 \cdot 10^8$ A/m^2, γ = -0.4, δ = 2.0 and B_{irr} = 4.25 T. In both cases, the computed curves well reproduce the experimental data. It is worthwhile to note that γ and δ values are very close and equal, respectively, to those calculated by Dew-Hugues [33] for vortex pinning by grain-boundaries, which is the main pinning source expected in a MgB_2 polycrystalline sample [35].

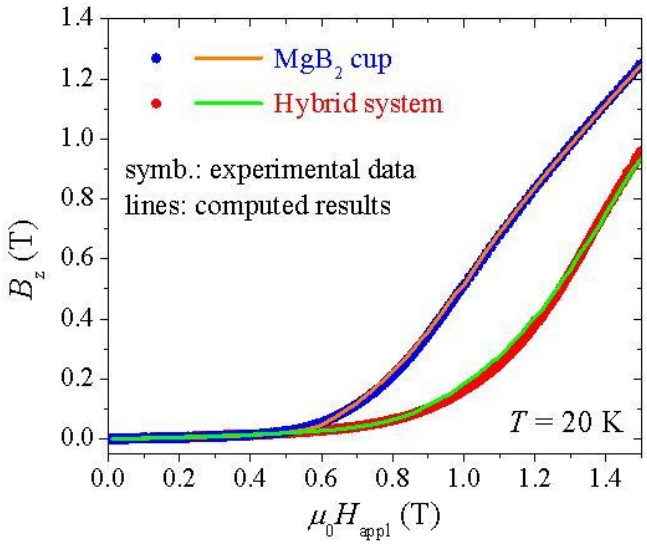

Figure 2. Comparison between the experimental induction fields and the numerical computation outputs in the superconducting and hybrid configurations as a function of the external applied field. Both experimental and computed data refer to a point on the cup axis placed inside the cups, at a distance of 5.5 mm from their edge.

The same agreement is shown by the comparison between the experimental and the calculated induction fields, evaluated as a function of the position along the cup axis. As an example, the B_z values obtained at $\mu_0 H_{appl}$ = 0.04, 0.2 and 1.0 T are shown in Figs. 3(a-c), together with the computed induction field distributions inside and around the superconducting cup (Figs. 3(d-f)) and the hybrid system (Figs. 3(g-i))

This agreement between the experimental and the calculated B_z values validates the use of the chosen approach in modeling the superconducting and ferromagnetic cup under study and allow us to exploit this method for the evaluation of the shielding properties of other SC/FM arrangements made out of the same materials and with similar shape and aspect ratio.

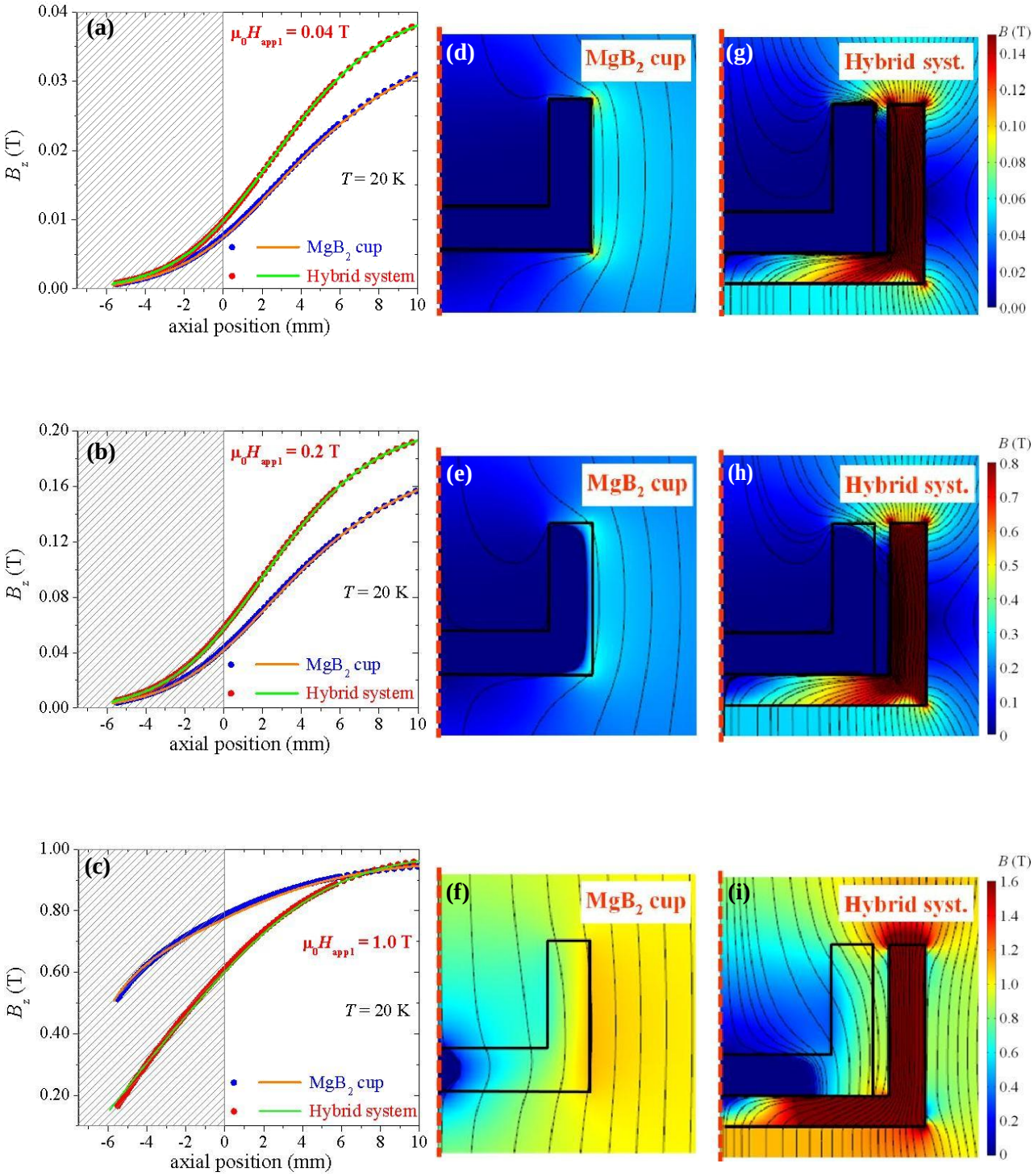

Figure 3. Comparison between the experimental induction fields (symbols) and the numerical computation outputs (lines) in the superconducting and hybrid configurations as a function of the position along the cup axis at $\mu_0 H_{appl}$ = 0.04 T (a), 0.2 T (b), 1.0 T (c). The zero position corresponds to the cup edge, while the hatched frame indicates the internal region of the cups. For each external field the computed magnetic induction maps in presence of the superconducting (d, e, f) and of the hybrid system (g, h, i) are reported. Taking into account the axisymmetric geometry only half of the cups is depicted.

It is worth noting that for applied external fields lower than $\mu_0 H_{appl}$ = 0.4 T the hybrid configuration show a lower shielding capability than the MgB_2 cup alone. This is a consequence of the aspect ratio chosen for the experiment. Indeed, the magnetic flux penetration through the cup opening is promoted by the presence of the ferromagnetic cup that, attracting the flux line within itself, induces a stronger curvature and a greater accumulation of the flux line at the cup edge. On the contrary, at higher magnetic fields where the flux penetration from the lateral wall becomes significant, the hybrid system shows a better shielding efficiency, as highlighted by the induction field map of Figs. 3(f) and 3(i).

4. Influence of the cup height and of lateral gap between them on the shielding properties of the SC/FM arrangements

With the aim to find hybrid SC/FM cup arrangements having the aspect ratio similar to that of the hybrid system experimentally characterized but improved shielding performances, we calculated and compared the induction field values along the axis of the SC/FM cup configurations sketched in Fig. 4. Firstly, we investigated separately the effect of the height of the FM cup and of the thickness of the lateral gap between the two cups, then on the basis of these results we changed both the parameters. In all the arrangements the sizes of the SC cup were kept unchanged. On the basis of the unsatisfactory results reported in [19] for the arrangements with the Fe tube placed inside the superconducting one, we disregarded configurations with an inner FM cup.

For the sake of visualization and in order to make a direct comparison with the superconducting cup, here we show the ratios between the shielding factor (SF) calculated for each hybrid systems and that one calculated for the superconducting cup alone. In turns, the SF was evaluated as the ratio of the applied magnetic field over the *z*-component of the induction field ($\mu_0 H_{appl} / B_z$).

In Figs 5 and 6 the results obtained at $\mu_0 H_{appl}$ = 0.04 T, 0.2 and 1.0 T are summarized. The magnetic field is mitigated all along the investigated segment of the cup axis, but in the following we will focus on its portion inside the SC cup (hatched frames in the graphs). Curves no. 1 always concern calculations on the arrangement no.1, shaped as the hybrid system checked experimentally (sketched in Fig. 1, right).

As shown in Fig. 5, keeping the lateral gap of 1.0 mm, the configuration no. 2, with the SC cup extending above the FM one, shows the best shielding efficiency at low applied fields ($\mu_0 H_{appl}$ = 0.04 T), with a significant recovering of the gap with the superconducting cup. On the contrary, at high magnetic field ($\mu_0 H_{appl}$ = 1.0 T) the higher height of the lateral wall of the Fe cup makes the configuration no. 3 the most suitable. The arrangements no. 4 and 5, having the edge of the SC and

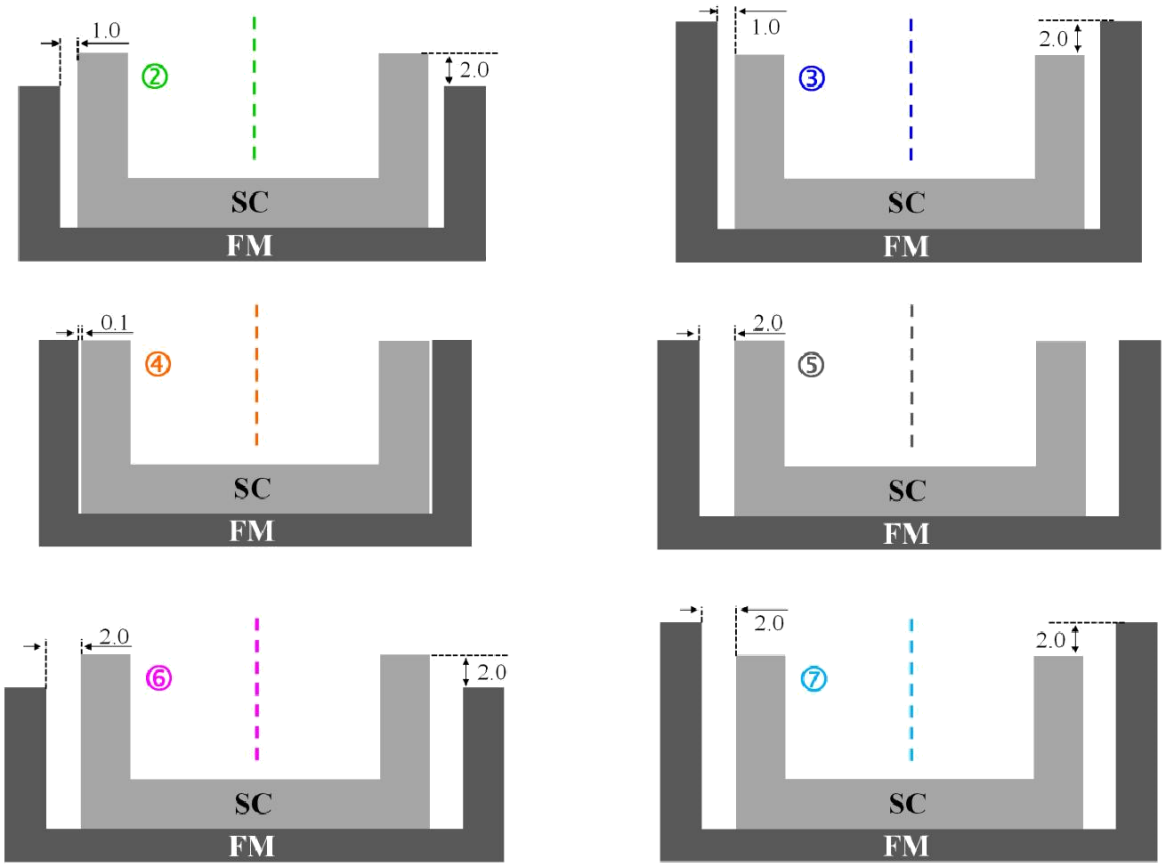

Figure 4. Schematic view of the SC/FM cup arrangements no. 2-7 used in the shielding simulations. All the sizes are in mm. The arrangement no. 1 (not shown in this figure) corresponds to the configuration characterized experimentally (see Fig. 1, right). In all the arrangements the sizes of the SC cup were kept unchanged and equal to those reported in Fig. 1 (left).

FM cup at the same level, show that an enlargement of the gap between the lateral walls of the two cups plays a positive role at low fields while it causes a worsening of the shielding potential at high fields (potential much better than that calculated for the single superconducting cup anyway). It is worth noting that the better performance of the arrangements no. 2, 3 and 5 than arrangement no. 1 at low-intermediate fields is accounted for by the reduced effect of the accumulation of the flux lines induced by the FM layer at the cup opening, which results a key factor for these systems with small aspect ratio. On the contrary, the higher shielding capability of all the hybrid systems at high applied fields is justified by the decrease of the magnetic flux density at the superconductor lateral/bottom external walls due to the presence of the FM cup.

Starting from these results, further simulations were carried out, changing both the gap between the lateral walls of the two cups and the height of the Fe cup (configuration no. 6 and 7) in order to check a possible additional improvement of the low field performance. Despite the SC cup is still the most efficient shield, at low applied field ($\mu_0 H_{appl}$ = 0.04 T) the joint effect of the enlargement

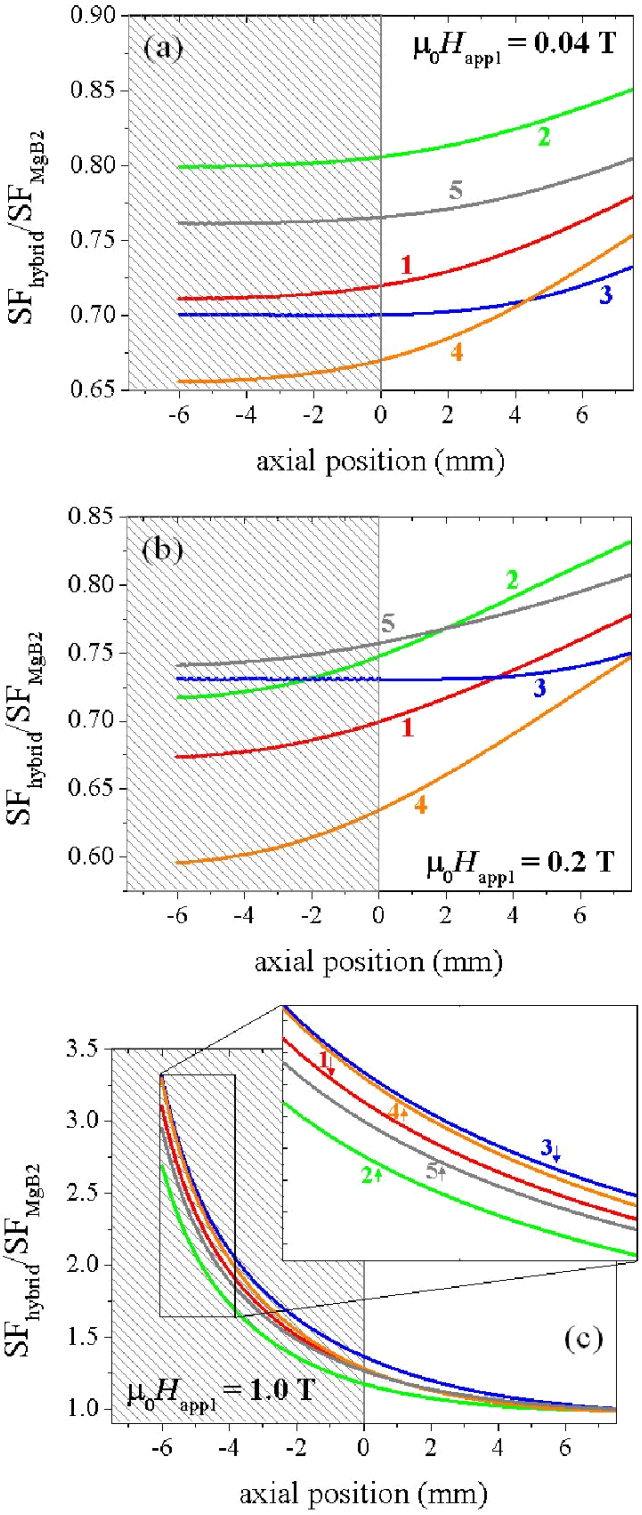

Figure 5. Comparison among the ratios SF_{hybrid}/SF_{MgB2} calculated for the cup arrangements no. 1-5 as a function of the position along the cup axis at $\mu_0 H_{appl}$ = 0.04 T (a), 0.2 T (b), 1.0 T (c). The numbers reported on the curves refer to the arrangement number (Fig. 4); the arrangement no. 1 is the hybrid arrangement characterized experimentally (Fig. 1). The zero position corresponds to the SC cup edge, while the hatched frame indicates the internal region of the SC cup.

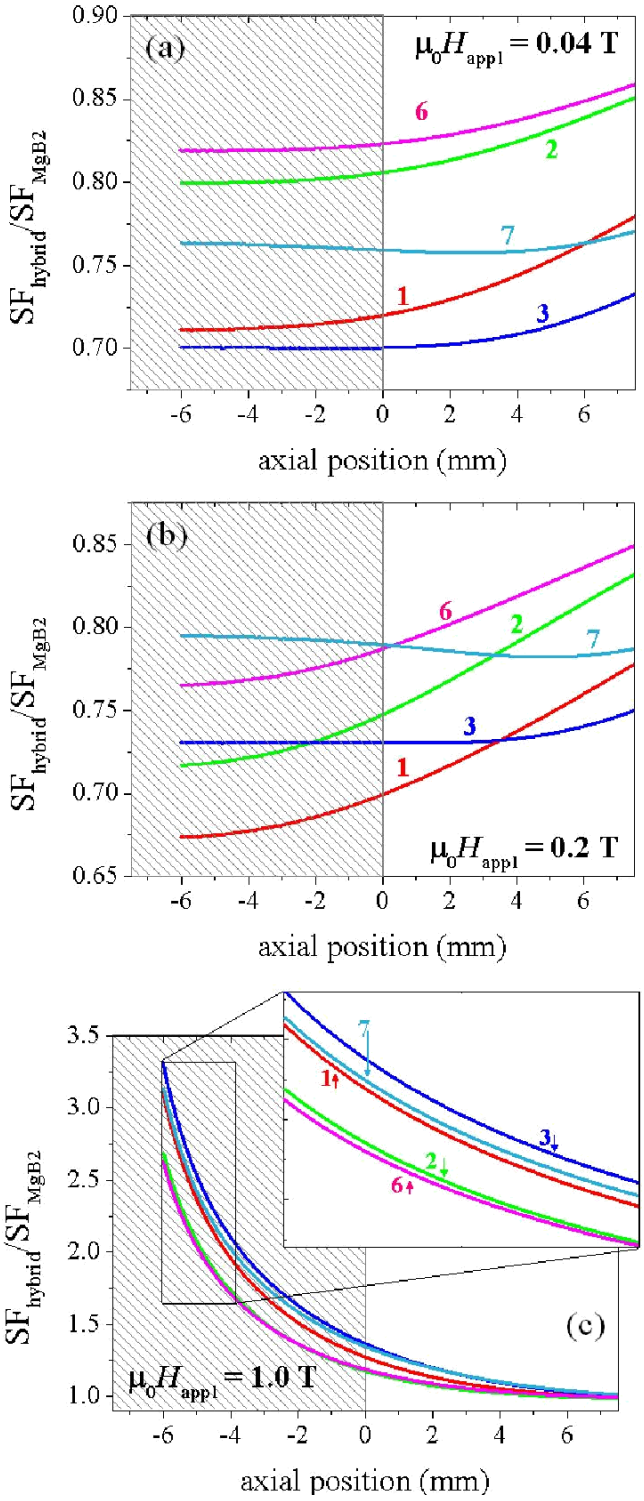

Figure 6. Comparison among the ratios SF_{hybrid}/SF_{MgB2} calculated for the cup arrangements no. 1, 2, 3, 6 and 7 as a function of the position along the cup axis at $\mu_0 H_{appl}$ = 0.04 T (a), 0.2 T (b), 1.0 T (c). The numbers reported on the curves refer to the arrangement number (Fig. 4); the arrangement no. 1 is the hybrid arrangement characterized experimentally (Fig. 1). The zero position corresponds to the SC cup edge, while the hatched frame indicates the internal region of the SC cup.

of the lateral space between the cups and of the protrusion of the SC cup over the FM one (arrangement no. 6) further reduces the gap between the superconducting and the hybrid solution, as displayed in Fig. 6(a). On the other hand, the arrangement with the largest distance between the cup lateral wall and the FM cup extending over the SC one (arrangement no. 7) becomes the most competitive hybrid system in the intermediate field range ($\mu_0 H_{appl}$ = 0.2 T – Fig. 6 (b)) and is still able to guarantee a shielding factor three times greater than that of the single SC cup at $\mu_0 H_{appl}$ =1.0 T (Fig. 6 (c)).

5. Conclusions

The shielding properties of hybrid superconducting/ferromagnetic systems consisting in cylindrical cups, coaxially mounted and with aspect ratio height/radius of about one, were investigated and compared with those of a single superconducting cup. The mitigation of the induction magnetic field along the cup axis was calculated as a function of the external applied field and of the position using an approach based on the vector potential formalism, validated for our systems by the comparison between experimental and computed data.

In such a geometry with a small aspect ratio, the hybrid arrangements turn out to be always the most efficient shielding solution at high fields, due to the reduction of the magnetic flux density on the external walls of the SC cup. In particular, at $\mu_0 H_{appl}$ = 1.0 T the highest shielding factor was found for solutions with the ferromagnetic cup protruding above the superconducting one.

On the contrary, the single superconducting cup remains the most suitable shield at low magnetic fields. A key factor to reduce the worsening of the shielding capability of the hybrid configurations at low fields is the reduction of the effect of flux line accumulation induced by the FM layer at the cup opening. This can be obtained with hybrid solutions having SC cup protruding over the FM one or vice-versa. In particular, the hybrid arrangement with the SC cup protruding above the FM one and an enlarged lateral gap resulted only slightly less performant than the single SC cup at low applied field ($\mu_0 H_{appl}$ = 0.04 T).

Starting from these results further analyses are ongoing in order to investigate the shielding performances of suitable-shaped SC/FM multilayered structures.

Acknowledgments

We wish to thank F. Gömöry for fruitful discussions and E. Bonometti for her help in the MgB_2 sample growth. This work was partially supported by the Italian National Institute of Nuclear Physics (INFN) under SR2S-RD experiment.

References

[1] Otsuka H and Itoh I 1994 *J. Appl. Phys.* **75** 6966-8.

[2] Kamiya K, Warner B A and DiPirro M J 2001 *Cryogenics* **41** 401-5.

[3] Nicolescu H, Schmidmeier R, Topolski B and Gielisse P J 1994 *Physica C* **229** 105.

[4] Denis S, Dusoulier L, Dirickx M, Vanderbemden Ph, Cloots R, Ausloos M and Vanderheyden B 2007 *Supercond. Sci. Technol.* **20** 192-201.

[5] Rabbers J J, Oomen M P, Bassani E, Ripamonti G and Giunchi G 2010 *Supercond. Sci. Technol.* **23** 125003.

[6] Gozzelino L, Agostino A, Gerbaldo R, Ghigo G and Laviano F 2012 *Supercond. Sci. Technol.* **25** 115013.

[7] Omura A, Oka M, Mori K and Itoh M 2003 *Physica C* **386** 506–11.

[8] Yasui K, Tarui Y and Itoh M 2006 *J. Phys.: Conf. Ser.* **43** 1393–6.

[9] Cybart S A, Wu S M, Anton S M, Siddiqi I, Clarke J and Dynes R C 2008 *Appl. Phys. Lett.* **93** 182502.

[10] Chiampi M, Gozzelino L, Manzin A and Zilberti L, 2011, *IEEE Trans. Magn.* **47** 4266-9.

[11] Gozzelino L, Gerbaldo R, Ghigo G, Laviano F, Agostino A, Bonometti E, Chiampi M, Manzin and A, Zilberti L 2013 *IEEE Trans. Appl. Supercond.* **23** 8201305.

[12] Narayana S and Sato Y 2012 *Adv. Mater.* **24** 71-4.

[13] Gömöry F, Solovyov M, Šouc J, Navau C, Prat-Camps J and Sanchez A 2012 *Science* **335** 1466–8.

[14] F Gömöry, M Solovyov and J Šouc 2015 *Supercond. Sci. Technol.* **28** 044001.

[15] Sirois F and Grilli F 2015 *Supercond. Sci. Technol.* **28** 043002.

[16] Farinon S, Iannone G, Fabbricatore P and Gambardella U 2014 *Supercond. Sci. Technol.* **27** 104005.

[17] Ainslie M D and Fujishiro H 2015 *Supercond. Sci. Technol.* **28** 053002.

[18] Das R, Oliveira F B, Guimaraes F G and Lowther D A 2014 *IEEE Trans. Magnetics* **50** 7006004.

[19] Lousberg G P, Fagnard J-F, Ausloos M, Vanderbemden P and Vanderheyden B 2010 *IEEE Trans. Appl. Supercond*. **20** 33–41.

[20] Genenko Y A, Rauh H and Krüger P 2011 *Appl.Phys. Lett.* **98** 152508.

[21] Philippe M P, Ainslie M D, Wéra L, Fagnard J-F, Dennis A R, Shi Y-H, Cardwell D A, Vanderheyden B and Vanderbemden P 2015 *Supercond. Sci. Technol.* **28** 095008.

[22] Campbell A M 2011 *J Supercond Nov Magn* **24** 27–33.

[23] Hong Z, Campbell A M and Coombs T A 2006 *Supercond. Sci. Technol.* **19** (2006) 1246-52.

[24] Barnes G, McCulloch M and Dew-Hughes D 1999 *Supercond. Sci. Technol.* **12** 518–22.

[25] Campbell A M 2007 *Supercond. Sci. Technol.* **20** 292-5.

[26] Campbell A M 2014 *Supercond. Sci. Technol.* **27** 124006.

[27] Gömöry F, Vojenčiak M, Pardo E and Šouc J 2009 *Supercond. Sci. Technol.* **22** 034017.

[28] Giunchi G, Ceresara S, Ripamonti G, Chiarelli S and Spadoni M 2003 *IEEE Trans. Appl. Supercond.* **13** 3060-3.

[29] Agostino A, Bonometti E, Castiglioni M, Volpe P, Truccato M, Manfredotti C, Olivero P, Paolini C, Rinaudo G and Gozzelino L 2003 *Int. J. Mod. Phys. B* **17** 773-8.

[30] Gozzelino L, Minetti B, Gerbaldo R, Ghigo G, Laviano F, Agostino A and Mezzetti E 2011 *IEEE Trans. Appl. Supercond.* **21** 3146-9.

[31] COMSOL 4.3b (http://www.comsol.com/).

[32] Kitahara K, Akune T, Matsumoto Y and Sakamoto N 2006 *Physica C* **445-8** 471.

[33] Dew-Hughes D 1974 *Philos. Mag.* **30** 293-305.

[34] M. Chiampi, *private communications*.

[35] Martínez E, Mikheenko P, Martínez-López M, Millán A, Bevan A and Abell J S 2007 *Phys. Rev. B* **75** 134515.